Nat Hazards
DOI 10.1007/s11069-014-1507-7

ORIGINAL PAPER

Spatial and temporal characteristics of droughts in the Northeast China Transect

Xiaoxue Wang · Huitao Shen · Wanjun Zhang · Jiansheng Cao · Yongqing Qi · Guopeng Chen · Xuyong Li

Received: 15 May 2014 / Accepted: 4 November 2014

Abstract In this study, drought trends and change magnitudes of the Northeast China Transect (NECT) were analyzed using the Mann–Kendall test and Theil–Sen's slope estimator. Meteorological data from 20 meteorological stations of NECT region from 1957 to 2012 were used. Results demonstrated that five stations had significant negative trends in precipitation. The magnitudes of the significant negative trends at the 95 % confidence level varied from -2.41 ± 1.05 mm year^{-1} at Tonghe station to -1.11 ± 0.51 mm year^{-1} at Qianguoerluosi station. Analysis of the seasonal precipitation series showed a mix of negative and positive trends. Many stations also exhibited strong contrasting seasonal trends that counterbalanced one other at the yearly level. In addition, cluster analysis based on discrete wavelet transform (DWT) was applied to the standard precipitation index (SPI) series. Results revealed three different and spatially well-defined subregions (east, center and west regions of NECT). Due to the decrease in precipitation from the east to the west, land use varies from forest regions in the east, to agriculture in the center, to pastoral areas in the west. Characteristics of drought events for each representative station of different subregions are explored using temporal evolution of the SPI values. Results showed that severe or extreme droughts occurred in 2001, 2003 and 2008 in Tonghe, 1980 and 2007 in Tongliao and 2005–2007 in East Ujimqin Banner. Results indicate that clustering analysis based on DWT

X. Wang · X. Li
State Key Laboratory of Urban and Regional Ecology, Research Center for Eco-Environmental Sciences, Chinese Academy of Sciences, Beijing 100085, China

X. Wang
University of Chinese Academy of Sciences, Beijing 100049, China

H. Shen (✉) · W. Zhang · J. Cao · Y. Qi
Key Laboratory of Agricultural Water Resources, Hebei Key Laboratory of Agricultural Water-Saving, Center for Agricultural Resources Research, Institute of Genetics and Developmental Biology, Chinese Academy of Sciences, No. 286, Huaizhong Road, Shijiazhuang 050021, China
e-mail: shenhuitao80@gmail.com

G. Chen
Institute of Forest Sciences, Bailongjiang Forestry Management Bureau, Lanzhou 730070, Gansu, China

Published online: 19 November 2014

has great potential for examining spatial coherence of regional drought, which was consistent with not only the precipitation spatial distribution but also the characteristics of land use in the study area. This study not only provides important information on drought variability in the NECT, but also provides useful information for improving water management strategies and planning agricultural practices.

Keywords Precipitation · Trend magnitude · Spatial–temporal characteristics · Cluster analysis · Standardized precipitation index

1 Introduction

Drought is one of the most poorly understood natural phenomena and is perceived as one of the most expensive. The occurrence of drought varies in frequency, severity and duration (Kao and Govindaraju 2010; Gocic and Trajkovic 2013). Trends in drought frequency and duration can be explained through changes in precipitation (Gocic and Trajkovic 2013). The spatial–temporal patterns of precipitation influence eco-hydrological processes and, consequently, regional economies that are strongly tied to agriculture and raising livestock (Guo et al. 2006; Liang et al. 2011; Zhang and Zhou 2010). A better understanding of precipitation and drought variability on a regional scale will assist in improving water management strategies, planning agricultural practices and protecting the environment (Liang et al. 2011).

Cluster analysis is a statistical technique in which structure in an unlabeled data set is identified and data are objectively organized into homogeneous groups, where the within-group-object dissimilarity is minimized and the between-group-object dissimilarity is maximized (Nourani et al. 2012). The use of clustering techniques in spatial and temporal patterns in climatic and meteorological research increased in recent decades. For instance, Santos et al. (2010) and Dinpashoh et al. (2004) used an algorithm that combined clusters analysis and PCA for dividing the research region into climate subregions. Since time series of precipitation are dynamic, certain non-stationary or chaotic properties may be embedded in the data, requiring appropriate methods to extract the features of interest (Hsu and Li 2010). Discrete wavelet transform (DWT) is well suited to the study of multi-scale and non-stationary precipitation properties over finite spatial and temporal domains (Aldrich 2012; Kumar and Foufoula-Georgiou 1997; Nalley et al. 2012). Partal and Küçük (2006) suggested that DWT plays an important role in analyzing precipitations data as its local analysis and multi-resolution decomposition make the analysis process more efficient and accurate. Considering the dynamic characteristics and non-uniform distribution of precipitation data and the need for homogeneous regions in water resource management, cluster analysis based on DWT is employed for exploring the temporal–spatial characteristics of drought time series.

Terrestrial transect has become an important and effective for the study of global change (Zhu et al. 2006). The Northeast China Transect (NECT) is identified as a mid-latitude semiarid terrestrial transect by the International Geosphere–Biosphere Programme (IGBP) (Ni and Zhang 2000), which is mainly driven by precipitation, and has become an effective platform for the global change research in China (Nie et al. 2012; Zhou et al. 2002; Zhu et al. 2006). Meanwhile, the NECT also represents an important base of forestry, agricultural and pastoral productions in China. Land across the NECT produces wood, hay, grain crops

(maize, soybean, wheat and rice) and cattle (leather, wool and milk) (Ni and Zhang 2000). Consequently, it is worthwhile to study the long-term time series of precipitation regarding the non-homogeneous climatic and hydrological conditions for water supply management and for crop and cattle productivity in this transect. However, a comprehensive analysis of trends and variability in drought series over the NECT is still lacking.

In this study, the analysis was based on 56 years (1957–2012) of precipitation data from 20 meteorological stations in the NECT region. One of the main objectives of the present study was to investigate the spatial distribution of temporal trends of the annual and seasonal precipitation time series using the Mann–Kendall and Theil–Sen's nonparametric methods. This study also aimed to identify the temporal patterns of droughts within each subregion identified by the spatial classification using standard precipitation index (SPI) values. A clustering analysis was used to explore the characteristics of SPI values for multiple time scales (1–12 months) for each cluster. Analyzing the variation of precipitation may lead to a better understanding of climate variability in the NECT and could be extended to similar semiarid/arid regions.

2 Data and methods

2.1 Precipitation data

Examination of climate changes requires long and high-quality records of climatic variables (Shifteh Some'e et al. 2012). In the present study, daily precipitation measurements from 20 meteorological stations in NECT were obtained from the China Meteorological Data Sharing Service System (http://cdc.cma.gov.cn/home.do). The China Meteorological Data Sharing Service System is the national authority responsible for collection and validation of hydrological data. Measurements at all of the meteorological stations were made using the same standards and instrumentation, ensuring homogeneity of data quality (Liu 2005). Spatial distribution of the 20 stations is shown in Fig. 1, and their characteristics and data availability are presented in Table 1.

2.2 Precipitation trend detection and change magnitude

2.2.1 Mann–Kendall test

The nonparametric Mann–Kendall (MK) test is routinely used to assess the increasing or decreasing trends in climate variables (Hanif et al. 2013). This test has the advantage of no assuming any form for the distribution function of the data, while having predictive power nearly as high as comparable parametric tests (Hanif et al. 2013). In this study, MK test was applied to all considered series to examine the annual and seasonal trends of precipitation in NECT of China. The MK test is given as:

$$S = \sum_{k=1}^{n-1} \sum_{j=k+1}^{n} \operatorname{sign}(x_j - x_k) \tag{1}$$

$$\operatorname{sign}(x_j - x_k) = \begin{cases} +1 & \text{if} \quad (x_j - x_k) > 0 \\ 0 & \text{if} \quad (x_j - x_k) = 0 \\ 1 & \text{if} \quad (x_j - x_k) < 0 \end{cases} \tag{2}$$

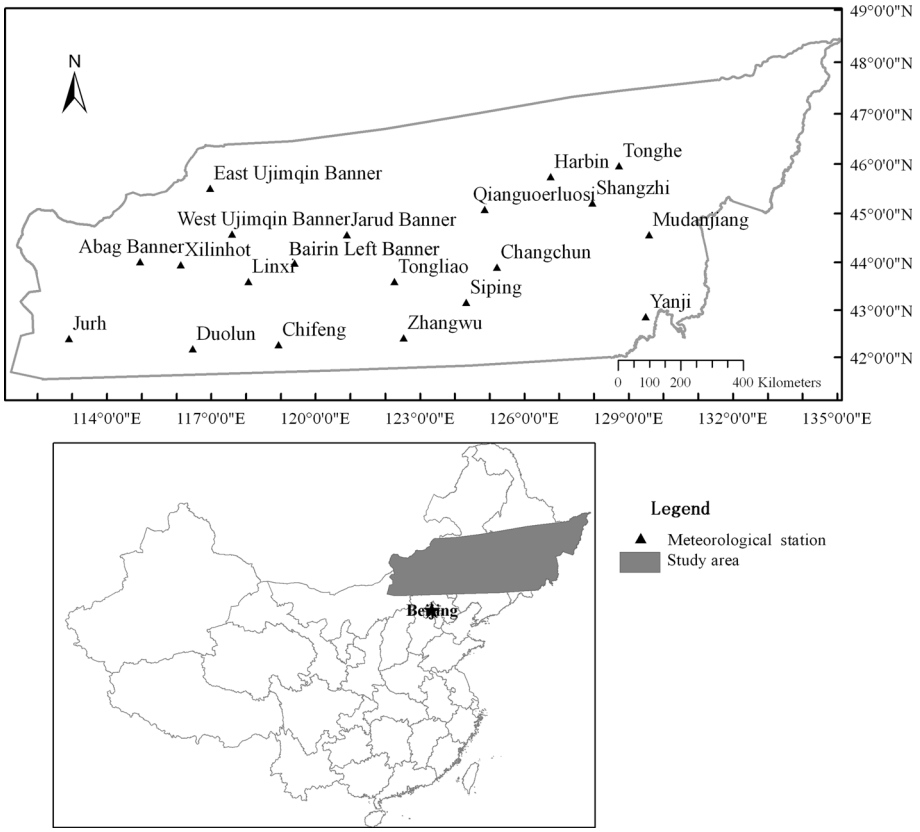

Fig. 1 Land use/cover of the study area and spatial distribution of meteorological stations

$$\mathrm{Var}(S) = \frac{[n(n-1)(2n+5)] - \sum_{i=1}^{m} t_i(t_i-1)(2t_i+5)}{18} \tag{3}$$

where n is the number of data points, t_i is the number of ties for the i value and m is the number of tied values. Equations (1) and (3) were used to compute the test statistic Z from the following equation:

$$Z = \begin{cases} \dfrac{S-1}{\sqrt{\mathrm{Var}(S)}} & \text{if} \quad S > 0 \\ 0 & \text{if} \quad S = 0 \\ \dfrac{S-1}{\sqrt{\mathrm{Var}(S)}} & \text{if} \quad S < 0 \end{cases}$$

A positive/negative value of Z indicates an upward/downward trend (Gocic and Trajkovic 2013). The null hypothesis H_0 that there is no trend in the records is either accepted or rejected depending if the computed Z statistics is less than or more than the critical value of the Z statistics obtained from the normal distribution table at the 5 % significance level (Shifteh Some'e et al. 2012).

Table 1 Geographical descriptions of the meteorological stations used in the study

Station name	Longitude (E)	Latitude (N)	Elevation (m)	Precipitation (mm)	Temperature (°C)	Predominant land use[a]
Harbin	45°45′	126°46′	142.3	533	4.3	Residential/Urban and Cropland
Tonghe	45°58′	128°43′	108.6	590	2.7	Residential/Urban and Wetland
Shangzhi	45°13′	127°58′	189.7	658	2.9	Residential/Urban
Mudanjiang	44°34′	129°35′	241.4	545	4.2	Residential/Urban
Yanji	42°52′	129°30′	257.3	518	5.4	Forest and Cropland
Zhangwu	42°25′	122°31′	79.4	513	7.6	Forest and Cropland
East Ujimqin Banner	45°31′	116°58′	838.9	254	1.4	Residential/Urban
Abag Banner	44°01′	114°57′	1,126.1	241	1.4	Residential/Urban and Meadow
Jurh	42°23′	112°54′	1,150.8	216	5	Residential/Urban and Meadow
West Ujimqin Banner	44°34′	117°35′	1,000.6	337	1.6	Residential/Urban
Jarud Banner	44°34′	120°54′	265.0	375	6.6	Forest and Cropland
Bairin Left Banner	43°58′	119°24′	486.2	377	5.4	Residential/Urban and Cropland
Xilinhot	43°57′	116°07′	1,003	282	2.5	Residential/Urban
Linxi	43°36′	118°04′	799.5	377	4.8	Residential/Urban
Tongliao	43°36′	122°16′	178.7	380	6.6	Residential/Urban
Duolun	42°10′	116°28′	1,245.4	380	2.3	Residential/Urban
Chifeng	42°16′	118°55′	568.0	365	7.3	Residential/Urban and Wetland
Qianguoerluosi	45°04′	124°52′	136.2	435	5.2	Forest
Siping	43°10′	124°19′	165.7	629	6.5	Residential/Urban and Cropland
Changchun	43°53′	125°13′	236.8	586	5.5	Residential/Urban

[a] Land use within a 10 km radius of station

2.2.2 *Theil–Sen's estimator*

The slope of n pairs of data points was estimated using the Theil–Sen's estimator which is given by the equation (Santos et al. 2010):

$$\beta = \text{Median}\left(\frac{x_i - x_j}{t_i - t_j}\right) \tag{4}$$

where x_i and x_j are data values at times t_i and t_j $(i > j)$, respectively.

The slope calculated by the Theil–Sen's estimator is a robust estimate of the magnitude of a trend and has been widely used to identify the slope of the trend line in hydrological time series (Jhajharia et al. 2012).

2.2.3 Percent change

To compute percent change of annual and seasonal precipitation, the magnitude of the trend slope was determined by taking the natural log of the annual and seasonal precipitation data and determining the Sen's median estimator (Lehmann et al. 2005; Shifteh Some'e et al. 2012). The Sen's median estimator of the log-transformed annual and seasonal precipitation provides a nonparametric estimate of the percent change over the analysis period (Eq. (1)). The equation gives the trend magnitude in percent change over the analysis period (Lehmann et al. 2005).

$$\Delta Y = (e^{\beta} - 1)100t \tag{5}$$

where ΔY is the percent change of precipitation over period, β is the Theil–Sen's estimator of trend slope (Eq. (5)) and t is the length of trend period (years).

In this study, contours for trend maps were generated using an inverse distance weighted (IDW) algorithm with a power of 2.0 for each grid points, and data from locations within 232 km radius were used. For these operations, ArcGIS 9.3 software (Environmental Systems Research Institute [ESRI] Inc., Redlands, CA) was used.

2.3 Cluster analysis of drought via discrete wavelet transform (DWT)

SPI is a widely used drought index based on the probability of precipitation for multiple time scales (1–12 months) (Shahid 2008). To ascertain the variability of both spatial and temporal patterns for different types of droughts, the SPI was used at different time scales, namely at 1 (SPI1), 6 (SPI6) and 12 (SPI12) consecutive months. The detailed formulation of SPI series provided by Shahid (2008) was followed.

SPI6 time series, showing the precipitation over distinct seasons, were chosen to analyze the spatial patterns of drought in this study. Based on the calculated SPI6 data, DWT was conducted using the Symmlet-8 wavelets (Aldrich 2012). Some important features of DWT are as follows: (i) the wavelet spectra generated are in discrete steps and give a very compact representation of the signal; and (ii) results of transformations using DWT remove the redundant information within the wavelet coefficients in order to better identify drought characteristics contained in signals (Nalley et al. 2012). DWT adopts the following form (Partal and Küçük 2006):

$$\psi_{m,n}\left(\frac{t-\tau}{s}\right) = s_0^{-m/2}\psi\left(\frac{t - n\tau_0 s_0^m}{s_0^m}\right) \tag{6}$$

where Ψ denotes the mother wavelet; m and n are integers, which represents the amount of dilation (scale factor) and translation of the wavelet, respectively; s_0 denotes a dilation step whose value is unchanged and is greater than 1; and γ_0 symbolizes the location variable whose value is greater than zero. Generally, for practical reasons, the values for s_0 and γ_0 are chosen to be 2 and 1, respectively. This is the DWT dyadic grid arrangement (i.e., integer powers of two; logarithmic scaling of the translations and dilations). If a time series exhibits discrete properties, with a value of x_i, occurring at a discrete time t, the wavelet coefficient ($W\psi(m, n)$) for the DWT becomes (Partal and Küçük 2006; Nalley et al. 2012):

$$W_{m,n} = 2^{-m/2}\sum_{i=0}^{N-1} x_i \psi(2^{-m}i - n) \tag{7}$$

The wavelet coefficient for the DWT is calculated at scale $s = 2^{m}$ and location $\gamma = 2^{m}n$, revealing the variation of signals at different scales and locations (Partal and Küçük 2006; Nalley et al. 2012).

3 Results and discussion

3.1 Annual and seasonal trends of precipitation

Annual trends at individual stations were calculated using MK test in order to reveal temporal trends for different regions (Fig. 2). Both negative and positive trends were identified in annual precipitation data (Fig. 2a). The negative trends in the annual precipitation series were significant at 5 stations (Tonghe, Shangzhi, Qianguoerluo, Siping and Tongliao) in the eastern study area. The monsoon system together with the effects of topography could explain the significant trends seen at the five stations (Zhai et al. 2005). Based on the Theil–Sen's estimator, the magnitudes of the significant negative trends at the 95 % confidence level are in the range of -2.41 ± 1.05 mm year^{-1} at Tonghe station and -1.11 ± 0.51 mm year^{-1} at Qianguoerluosi station. Increased precipitation trends were only observed at the Chifeng and Yanji stations. A 0–10 % decrease in precipitation in most areas of NECT (Fig. 2a) indicates that dry conditions have increased over the last 50 years. Furthermore, rising temperature has increased surface evaporation prompting more drying across NECT. The decreasing precipitation trends in this study corroborate results in northern China obtained by the linear fitted model of Ding et al. (2007) and Wang and Zhou (2005). However, a report published by IPCC (2007) stated that precipitation has increased throughout the twentieth century between latitude 30 and 85°N. This is inconsistent with the findings of this study where a decreasing trend was observed in relation to precipitation in the NECT of China between 1957 and 2012.

The MK test was also applied to detect temporal trends of seasonal precipitation time series from the 20 stations during 1957–2012 (Fig. 2b–e). The majority of the trends in the spring precipitation time series were positive. The spatial distribution of the magnitude of spring precipitation trends showed that spring precipitation in western parts of the NECT region decreased by 0–10 % and more than 20 % at the Jurh station and increased in eastern parts by 0–10 % except for the Tonghe station. However, none of the trends were statistically significant (Fig. 2b). Summer is the wettest season accounting for 50–70 % of annual precipitation in most parts of the transect. This may explain the similarity between annual and summer spatial patterns of precipitation trends. A significant trend was only found at the Tongliao station (Fig. 2c). Autumn precipitation trends were negative for the whole area, and the Shangzhi, Jarud Banner and Changchun stations were all significant at the 95 % confidence level (Fig. 2d). In contrast to the other seasonal series, most of the trends in winter precipitation were positive accounting for 75 % of the stations. Significant trends were detected at East Ujimqin Banner, Harbin and Shangzhi stations (Fig. 2e). In addition, many stations also exhibited strong contrasting seasonal trends that counterbalanced each other at a yearly level. The most striking example was observed at the Shangzhi station where a strong negative trend observed in the autumn season was compensated by a strong positive trend at the onset of the winter season. This may be an indication that the contrast between dry and wet periods exacerbates in some regions.

During the study period, winter precipitation in most parts of the NECT increased by 10 % or more. Winter precipitation trends were opposite to annual trends, which demonstrate the insignificant role of winter precipitation in annual precipitation. Most western

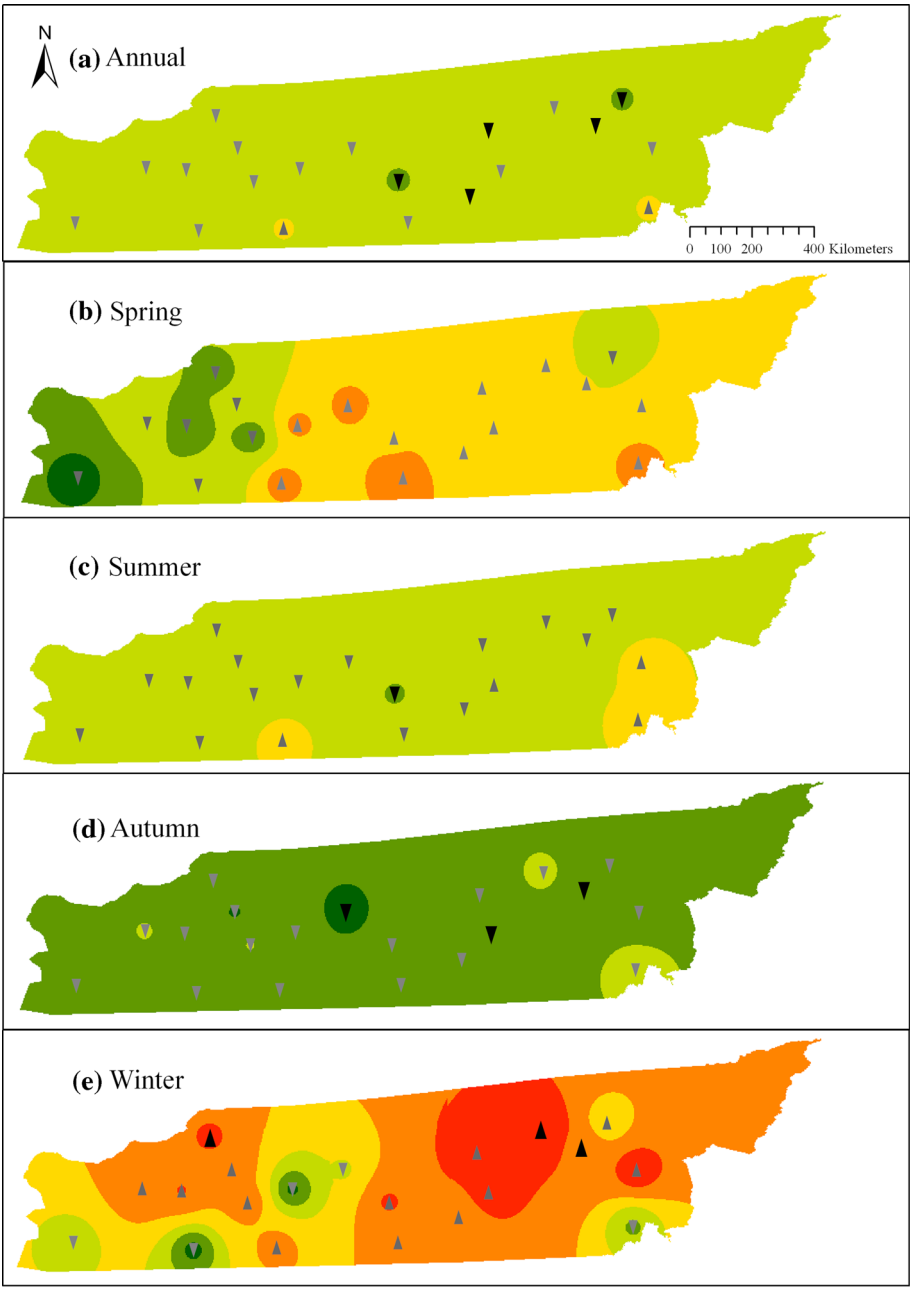
N
(a) Annual
0 100 200 400 Kilometers
(b) Spring
(c) Summer
(d) Autumn
(e) Winter
Trend
Decreasing ▼ No Sig. ▼ 95% Sig.
Increasing ▲ No Sig. ▲ 95% Sig.
Percent Change (%) 1957-2012
<-20
-20 - -10
-10 - 0
0 - 10
10 - 20
>20

◀**Fig. 2** Percent change for the annual and seasonal precipitation from 1957 to 2012, upward and downward trends marked with the Mann–Kendall test: **a** annual (January–December); **b** spring (February–April); **c** summer (May–July); **d** autumn (August–October); **e** winter (November–January)

parts of NECT are pastoral areas. Decreasing spring precipitation in these areas could result in the reduction of pasture yields and thus influence the success of livestock. The eastern parts of the study area are an important base of agricultural productions in China. Increasing spring precipitation in eastern areas of NECT might promote the growth of crops. However, the decline of autumn precipitation, accounting for much of the decreasing annual precipitation trends, will have little influence of crops production.

3.2 Cluster analysis: spatial variability of droughts

The original SPI6 time series were passed through high-pass and low-pass filters and separated at different scales. The time series was then divided into the approximate trend (above part of each scale) and the high frequencies and the fast event (below part of each scale), as shown in Fig. 3. It is more efficient and accurate to use powers of one to replace calculating every scale of wavelet coefficients of SPI6. The detail coefficients of sub-time series were obtained using Eq. 7. The corresponding detail of SPI6 time series ($m = 1$ and $n = -2$) was selected for cluster analysis. This is because it tends to represent the finer, more high-frequency nature of drought conditions (Percival and Walden 2006).

The regional drought analysis is useful for determining the spatial distribution and characteristics of drought and evaluating the most affected areas for a specific drought event (Gebrehiwot et al. 2011). Results showed that the NECT region can be divided into three subregions, suggesting that the cluster analysis method can identify spatial areas with different temporal precipitation patterns (Fig. 4). In the eastern region (cluster 1), mean annual precipitation (MAP) was determined to be 533–658 mm. Most of these regions are woodland; however, at lower elevation, both agriculture and forestry practices exist. In the central region (cluster 2), farming and forest farms coexist, with an MAP of between 365 and 629 mm. In the western region (cluster 3) known as the Inner Mongolia Plateau, animal husbandry is the main economy. MAP ranges from 216 to 380 mm. Results indicate that clustering analysis based on DWT has great potential for examining spatial patterns of regional drought.

NECT acts as an effective platform for investigating of the influences of water on land use in terrestrial ecosystems (Ni and Zhang 2000; Nie et al. 2012). The physiognomy of vegetation is closely related to the distribution of water, which determines the spatial patterns of land use on a large scale (Zhang and Zhou 2010). Along the NECT, land use changes from forests to grasses with decreasing water availability from east to west (Fig. 4). At present, large areas of grassland and forest were converted to agricultural fields, destroying much of the natural environment in this area (Ni and Zhang 2000). In addition to altering ecosystem services, the conversion of forest or grassland to cropland alters the hydrological cycle over a range of scales (Anav et al. 2010; Otieno and Anyah 2012; Pitman 2004). The biogeophysical impacts of this conversion on the surface energy balance include a large reduction in latent heat flux, a small reduction in net radiation and a moderate increase in sensible heat flux and surface energy storage (Bagley et al. 2014). This shift in the surface energy balance alters the atmospheric boundary layer, which can influence regional drought depending on the scale of conversion. Moreover, the expected increases in water demands and soil moisture deficit and decreases in precipitation have a

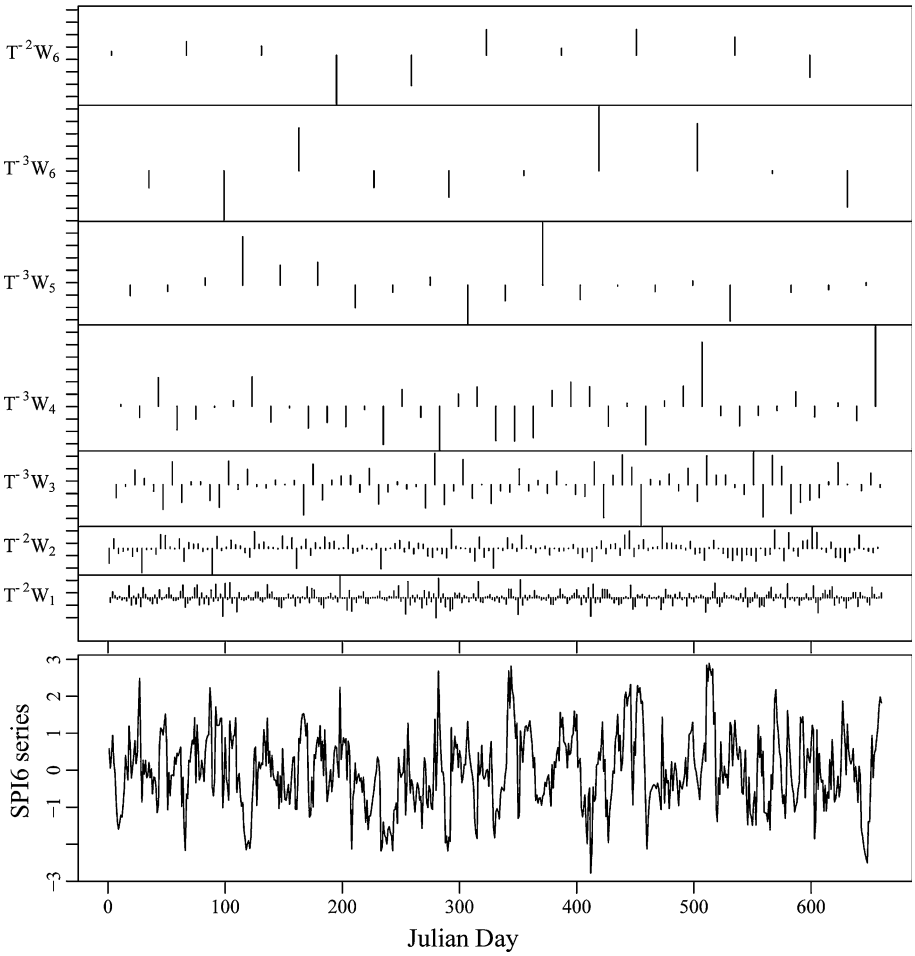

Fig. 3 Discrete wavelet transformations of the SPI6 time series using the Symmlet-8 wavelets at different scales and positions

major impact on the hydrological cycle and consequently on the potential for regional drought (Tao et al. 2003). The results of this study may facilitate forecasting the effects of human-induced climatic change in NECT region.

3.3 Temporal drought patterns

Meteorological drought is a deficiency of precipitation in a given region (Gebrehiwot et al. 2011). Precipitation amount and variability vary greatly from one station to another. Moreover, the human eye is easily fooled by randomness in time series data. One way to address these issues is to replace the observed (highly non-normal and seasonally varying) rainfall amounts by SPI time series of multiple time steps. Plotting SPI as a function of both time and time scale can provide insight into droughts at a particular location.

Drought occurs when SPI is negative and its intensity is −1.0 or lower. The duration of every drought is determined by negative index values. Accumulated totals of negative

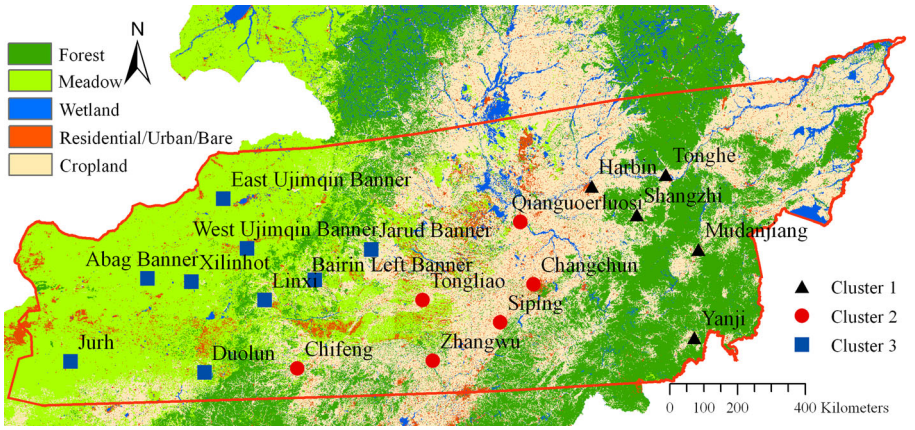

Fig. 4 Spatial clusters of the stations based on SPI6

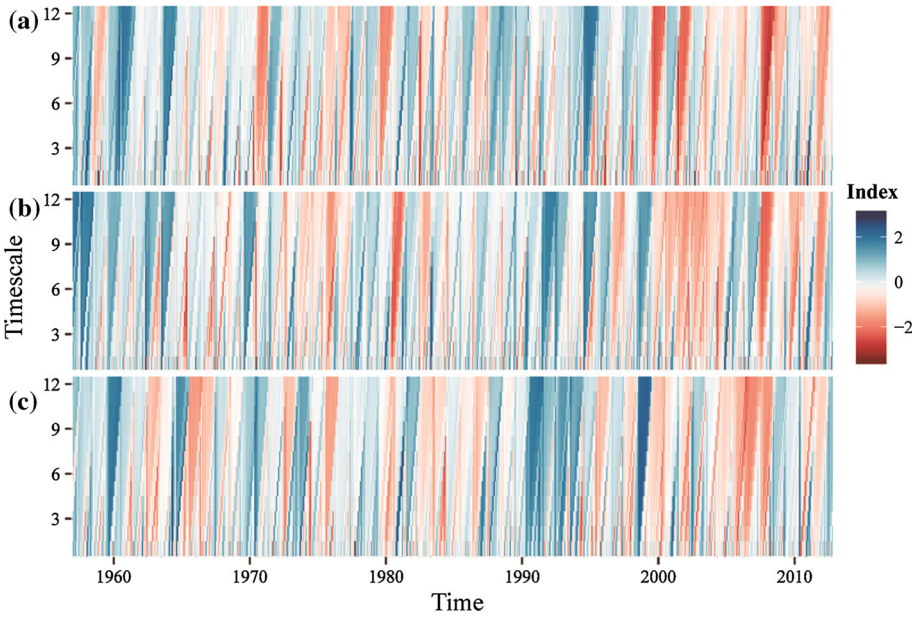

Fig. 5 Values of 12-month spatial precipitation index for the representative station in each cluster from 1957 to 2012 (**a** Tonghe, **b** Tongliao, **c** East Ujimqin Banner)

values of SPI can also be used as a measure of drought severity (Gebrehiwot et al. 2011). In this study, a representative sample of the evolution of the SPI with significant annual or seasonal precipitation trends was selected in each cluster (Tonghe in cluster 1, Tongliao in cluster 2 and East Ujimqin Banner in cluster 3). The evolution of the SPI for the three stations between 1957 and 2012 with a time scale of 1–12 months is shown in Fig. 5. According to the criteria of Svoboda et al. (2012), severe and extreme droughts correspond to the categories of $-1.99 < \text{SPI} \leq -1.5$ and $\text{SPI} \leq -2.0$, respectively.

The analysis showed that in 2001, 2003 and 2008 extreme drought events occurred in Tonghe, as all SPI1-12 values were <-3.03. Annual precipitation in 2001 was the lowest over the 56-year time periods (Fig. 5a). At the Tongliao station, successive moderate drought episodes were recorded from 2000 to 2003 at different time scales. The annual SPI1, SPI6 and SPI12 were -0.23, -0.71 and -1.16, respectively. In addition, two extreme drought events (1980 and 2007) lasted 9–13 months resulting in a critical and extreme situation (Fig. 5b). Extreme drought events were also observed in East Ujimqin Banner, lasting 3 years. Of all the drought events, the minimum SPI12 occurred in summer 2006 (SPI12 $= -2.70$), and the minimum 6-month SPI was observed in 2008 (SPI6 $= -2.41$) (Fig. 5c). The temporal analyses of SPI1–SPI12 values showed that NECT regions were predominantly characterized by frequent moderate droughts.

4 Conclusion

In this study, the Mann–Kendall trend test and Theil–Sen's slope estimator were used to investigate the spatial–temporal trends of precipitation data from 20 meteorological stations in NECT from 1957 to 2012. Five stations had statistically significant negative trends in annual precipitation, ranging from -2.41 ± 1.05 mm year^{-1} at Tonghe station to -1.11 ± 0.51 mm year^{-1} at Qianguoerluosi station at the 95 % confidence level. The spatial distribution of the annual precipitation trends indicated that the significant negative trends mostly occurred in the eastern part of NECT and decreased by 0–10 % or more. Analysis of seasonal precipitation series showed a mix of negative and positive trends. Three significant negative trends in autumn and three significant positive trends in winter were the greatest compared with those in the other seasonal series. Autumn precipitation had decreasing trends everywhere in the study region. Summer precipitation had only one significant negative trend at the Tongliao station where no significant trends were detected in spring precipitation.

Considering the dynamic characteristics and non-uniform distribution of precipitation, and the need for homogeneous regions for effective water resource management, cluster analysis based on DWT is employed for exploring the temporal–spatial characteristics of drought time series. The drought events were characterized by SPI6 values. This study shows that the NECT can be divided into three subregions (the east, the center and the west), which was consistent with not only the precipitation decreasing from east to west but also the characteristics of land use in the NECT region. Tonghe in the east, Tongliao in the center and East Ujimqin Banner in the west were selected to evaluate the temporal patterns of 1- to 12-month SPI in each subregion. Several severe or extreme drought episodes were detected from the temporal evaluation of the SPI values of each representative station, e.g., 2001, 2003 and 2008 in Tonghe, 1980 and 2007 in Tongliao and 2005–2007 in East Ujimqin Banner, respectively.

Acknowledgments We thank the China Meteorological Data Sharing Service System for providing the required precipitation data of the various stations. This work was funded jointly by the Project of China CDM Fund (Grant No: 1214115), the Special Foundation from State Key Laboratory of Urban and Regional Ecology (Grant No: SKLURE2012-1-05), the National Natural Science Foundation of China (Grant No: 41001060) and the National Science and Technology Plan (Grant No: 2011BAD31B02). The authors gratefully acknowledge the Editor-in-Chief Professor Thomas Glade and two anonymous reviewers for comments on precious versions of this article. The authors are also grateful to Alison Beamish from University of British Columbia for his assistance with improving the language of the manuscript.

References

Aldrich E (2012). Wavelets: a package of functions for computing wavelet filters, wavelet transforms and multiresolution analyses. http://CRAN.R-project.org/package=wavelet

Anav A, Ruti PM, Artale V, Valentini R (2010) Modelling the effects of land-cover changes on surface climate in the Mediterranean region. Clim Res 41:91–104

Bagley JE, Desai AR, Harding KJ, Snyder PK, Foley JA (2014) Drought and deforestation: has land cover change influenced recent precipitation extremes in the Amazon? J Clim 27:345–361

Ding YH, Ren GY, Zhao ZC, Xu Y, Luo Y, Li QP, Zhang J (2007) Detection, causes and projection of climate change over China: an overview of recent progress. Adv Atmos Sci 24:954–971

Dinpashoh Y, Fakheri-Fard A, Moghaddam M, Jahanbakhsh S, Mirnia M (2004) Selection of variables for the purpose of regionalization of Iran's precipitation climate using multivariate methods. J Hydrol 297:109–123

Gebrehiwot T, van der Veen A, Maathuis B (2011) Spatial and temporal assessment of drought in the Northern highlands of Ethiopia. Int J Appl Earth Obs 13:309–321

Gocic M, Trajkovic S (2013) Analysis of precipitation and drought data in Serbia over the period 1980–2010. J Hydrol 494:32–42

Guo R, Wang XK, Ouyang ZY, Li YN (2006) Spatial and temporal relationships between precipitation and ANPP of four types of grasslands in northern China. J Environ Sci 18:1024–1030

Hanif M, Khan AH, Adnan S (2013) Latitudinal precipitation characteristics and trends in Pakistan. J Hydrol 492:266–272

Hsu KC, Li ST (2010) Clustering spatial–temporal precipitation data using wavelet transform and self-organizing map neural network. Adv Water Resour 33:190–200

IPCC (2007) Climate change 2007: synthesis report. In: Pachauri RK, Reisinger A (eds) Contribution of working groups I, II and III to the fourth assessment report of the intergovernmental panel on climate change. IPCC, Geneva, Switzerland, p 104

Jhajharia D, Dinpashoh Y, Kahya E, Singh VP, Fakheri-Fard A (2012) Trends in reference evapotranspiration in the humid region of northeast India. Hydrol Process 26:421–435

Kao SC, Govindaraju RS (2010) A copula-based joint deficit index for droughts. J Hydrol 380:121–134

Kumar P, Foufoula-Georgiou E (1997) Wavelet analysis for geophysical applications. Rev Geophys 35:385–412

Lehmann C, Bowersox VC, Larson SM (2005) Spatial and temporal trends of precipitation chemistry in the United States, 1985–2002. Environ Pollut 135:347–361

Liang L, Li L, Liu Q (2011) Precipitation variability in Northeast China from 1961 to 2008. J Hydrol 404:67–76

Liu B (2005) Observed trends of precipitation amount, frequency, and intensity in China, 1960–2000. J Geophys Res 110. doi:10.1029/2004jd004864

Nalley D, Adamowski J, Khalil B (2012) Using discrete wavelet transforms to analyze trends in streamflow and precipitation in Quebec and Ontario (1954–2008). J Hydrol 475:204–228

Ni J, Zhang XS (2000) Climate variability, ecological gradient and the Northeast China Transect (NECT). J Arid Environ 46:313–325

Nie Q, Xu J, Ji M, Cao L, Yang Y, Hong Y (2012) The vegetation coverage dynamic coupling with climatic factors in Northeast China Transect. Environ Manage 50:405–417

Nourani V, Baghanam AH, Vousoughi FD, Alami M (2012) Classification of groundwater level data using SOM to develop ANN-based forecasting model. Int J Soft Comput Eng 2:464–469

Otieno VO, Anyah RO (2012) Effects of land use changes on climate in the Greater Horn of Africa. Clim Res 52:77–95

Partal T, Küçük M (2006) Long-term trend analysis using discrete wavelet components of annual precipitations measurements in Marmara region (Turkey). Phys Chem Earth 31:1189–1200

Percival DB, Walden AT (2006) Wavelet methods for time series analysis, vol 4. Cambridge University Press, Cambridge

Pitman AJ (2004) Impact of land cover change on the climate of southwest Western Australia. J Geophys Res 109:D18109. doi:10.1029/2003JD004347

Santos JF, Pulido-Calvo I, Portela MM (2010) Spatial and temporal variability of droughts in Portugal. Water Resour Res 46. doi:10.1029/2009wr008071

Shahid S (2008) Spatial and temporal characteristics of droughts in the western part of Bangladesh. Hydrol Process 22:2235–2247

Shifteh Some'e B, Ezani A, Tabari H (2012) Spatiotemporal trends and change point of precipitation in Iran. Atmos Res 113:1–12

Svoboda M, Hayes M, Wood D (2012) Standardized precipitation index user guide. World Meteorological Organization Geneva, Switzerland

Tao F, Yokozawa M, Hayashi Y, Lin E (2003) Future climate change, the agricultural water cycle, and agricultural production in China. Agr Ecosyst Environ 95:203–215

Wang YQ, Zhou L (2005) Observed trends in extreme precipitation events in China during 1961–2001 and the associated changes in large-scale circulation. Geophys Res Lett 32:L09707. doi:10.1029/2005GL022574

Zhai P, Zhang X, Wan H, Pan X (2005) Trends in total precipitation and frequency of daily precipitation extremes over China. J Clim 18:1096–1108

Zhang Y, Zhou G (2010) Exploring the effects of water on vegetation change and net primary productivity along the IGBP Northeast China Transect. Environ Earth Sci 62:1481–1490

Zhou G, Wang Y, Wang S (2002) Responses of grassland ecosystems to precipitation and land use along the Northeast China Transect. J Veg Sci 13:361–368

Zhu WQ, Pan YZ, Liu X, Wang AL (2006) Spatio-temporal distribution of net primary productivity along the Northeast China Transect and its response to climatic change. J For Res 17:93–98